Available online at www.sciencedirect.com

ScienceDirect

journal homepage: www.elsevier.com/locate/he

Comparative study of energy management systems for a hybrid fuel cell electric vehicle - A novel mutative fuzzy logic controller to prolong fuel cell lifetime

Robert Luca [a], *Michael Whiteley* [a,b], *Toby Neville* [a], *Paul R. Shearing* [a,b,c], *Dan J.L. Brett* [a,b,c,*,1]

[a] *Electrochemical Innovation Lab, Department of Chemical Engineering, University College London, WC1E 7JE, UK*
[b] *Advanced Propulsion Lab, UCL East, University College London, London, E15 2JE, UK*
[c] *The Faraday Institution, Quad One, Becquerel Avenue, Harwell Campus, Didcot, OX11 0RA, UK*

HIGHLIGHTS

- Comparison of energy management systems for hybrid fuel cell/battery vehicles.
- Mutative Fuzzy Logic Controller prolongs fuel cell lifetime.
- Reducing H2 consumption can degrade performance.

GRAPHICAL ABSTRACT

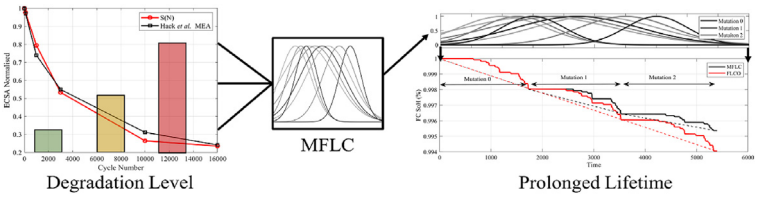

ARTICLE INFO

Article history:
Received 10 December 2021
Received in revised form
4 April 2022
Accepted 20 May 2022
Available online xxx

Keywords:
Hybrid
Fuel cell vehicle
Energy management system
Fuzzy logic
ECMS
Battery modelling

ABSTRACT

Hybrid fuel cell battery electric vehicles require complex energy management systems (EMS) in order to operate effectively. Poor EMS can result in a hybrid system that has low efficiency and a high rate of degradation of the fuel cell and battery pack. Many different types of EMS have been reported in the literature, such as equivalent consumption minimisation strategy and fuzzy logic controllers, which typically focus on a single objective optimisations, such as minimisation of H_2 usage. Different vehicle and system specifications make the comparison of EMSs difficult and can often lead to misleading claims about system performance. This paper aims to compare different EMSs, against a range of performance metrics such as charge sustaining ability and fuel cell degradation, using a common modelling framework developed in MATLAB/Simulink - the Electric Vehicle Simulation tool-Kit (EV-SimKit). A novel fuzzy logic controller is also presented which mutates the output membership function depending on fuel cell degradation to prolong fuel cell lifetime – the Mutative Fuzzy Logic Controller (MFLC). It was found that while certain EMSs may perform well at reducing H_2 consumption, this may have a significant impact on fuel cell degradation, dramatically reducing the fuel cell lifetime. How the behaviour of common EMS results in fuel cell degradation is also explored. Finally, by

* *Corresponding author.*
E-mail address: d.brett@ucl.ac.uk (D.J.L. Brett).
[1] Web: www.ucl.ac.uk/electrochemical-innovation-lab.

https://doi.org/10.1016/j.ijhydene.2022.05.192

mutating the fuzzy logic membership functions, the MFLC was predicted to extend fuel cell lifetime by up to 32.8%.

Introduction

The need to electrify the transport sector has never been clearer or more urgent. Transportation has a 72.1% share of oil products according to the International Energy Agency (IEA) [1], which when burnt drives irreversible anthropogenic climate change. The policies of governments around the world are evolving to tackle this challenge. For example, the UK Government has just brought forward its ban on non-hybridised internal combustion engine vehicles by 10 years—2030. Lithium-ion battery technology has evolved to meet the requirements of many transport applications, particularly light-duty needs [2]. However, battery electric vehicles (BEVs) struggle with applications where long-range, heavier-duty and rapid recharging are paramount. Fuel cells operating on hydrogen fuel are less advanced technology but have advantages over Li-ion batteries that include greater range and refuelling speed. On the other hand, fuel cells cannot accept regenerative braking, are less dynamically responsive, and do not have a sufficiently developed refuelling infrastructure. Unfortunately, fuel cells and batteries are often portrayed as competing technologies where one will 'win' over the other. Instead, the two should be considered as complementary technologies; each deployable from a stable of electrochemical power sources (which includes supercapacitors and a range of battery and fuel cell types) to suit the needs of different applications, either individually or combined (hybridised) in such a way as to derive the best features from each.

Hybrid systems

A well-designed hybrid system, composed of two or more power sources, has the potential to be much more versatile, allowing it to be applied to many different vehicle sizes and types. Such hybrid systems can be optimised for different attributes or combinations of attributes; for example, weight, volume, dynamic response, efficiency, durability, cost, etc. When designed well, such systems can have a transformative impact compared to single-source systems. However, poorly designed hybrids can needlessly add to system complexity and cost and even result in an inferior overall solution. Consequently, hybrid power system design is an area of intense research that considers control aspects, development of energy management systems (EMS) and the electrical, thermal and physical integration.

While there are many benefits to power source hybridisation, the basic concept behind hybridising a fuel cell with a battery is that it enables the fuel cell to act as the primary energy source (based on the use of a chemical fuel) operating in the maximum efficiency range, while the battery accommodates dynamic response, meets the peak power demand and recuperates energy from regenerative braking. Operating the system this way has also been shown to be more efficient than using the fuel cell as a range extender [3]. This is partly because fuel cells operate best under steady loads, ideally at partial load where the efficiency is highest, and passing energy through the battery pack is approximately 95—98% efficient [4,5]. It is worth mentioning an alternative low carbon method of electricity generation which is the direct combustion of hydrogen within a micro-thermophotovoltaic device [6—8]. These devices have the possible application of providing small amounts of auxiliary power, particularly for electrical devices, without reducing the battery state-of-charge.

Passive or active hybridisation

Broadly, hybrid systems can be characterised as active or passive systems. Active systems typically use a DC/DC converter to step up the fuel cell voltage to the battery system. Passive systems connect the fuel cell and battery system in parallel; therefore, their voltages are intrinsically linked, removing the need for DC/DC converters which add to cost and have a conversion efficiency penalty [9]. While passive systems have been studied extensively and provide useful benefits [9—13], the analysis and model presented here will focus on active systems as this provides more flexibility and independence of system operational voltage for the energy management system.

Hybrid systems can be split into series or parallel configurations. Series systems typically represent a range extender arrangement, where the fuel cell is not directly connected to the electric motor. Parallel systems (Fig. 1) are more common. In this case, the fuel cell is connected to the DC bus via a unidirectional converter. The battery is connected via a bi-directional converter to keep the DC bus at a fixed voltage and allow for charging from regenerative braking or the fuel cell. The DC bus is connected to the motor via an inverter to convert the DC to AC, although not all electric motors require AC.

Operationally, a fuel cell is a highly sensitive system with a large number of failure modes such as membrane failures, gasket cracking, structural and system integration failures [5,14,15]. Furthermore, fuel cells rely on the distribution of gases with typical time constants on the order of seconds, limiting their dynamic response capability. Large load transients can lead to fuel or oxygen starvation, which can impact durability [16]. Battery packs can also have thermal and operational difficulties, however, due to their maturity and research interest, innovations have been able to reduce these issues [17]. It is still the role of the EMS to limit operational

Please cite this article as: Luca R et al., Comparative study of energy management systems for a hybrid fuel cell electric vehicle - A novel mutative fuzzy logic controller to prolong fuel cell lifetime, International Journal of Hydrogen Energy, https://doi.org/10.1016/j.ijhydene.2022.05.192

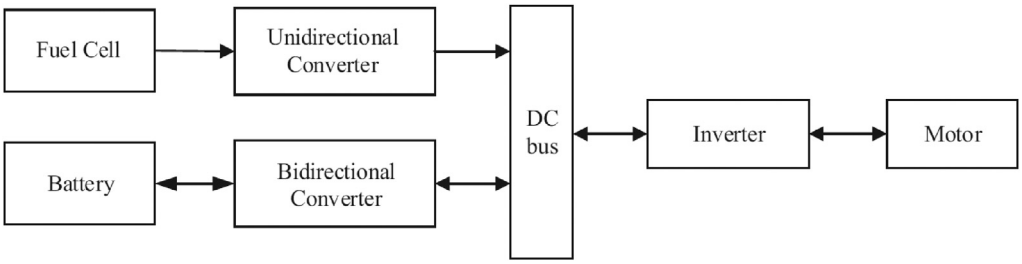

Fig. 1 – Configuration of active parallel fuel cell electric vehicle. Reproduced from [5].

conditions which reduce the lifetime of the system and the vehicle efficiency.

Energy management controllers

There have been many studies performed on EMS within the literature. They typically focus on a single objective such as minimisation of fuel cell degradation or fuel consumption. However, while there are examples focused on electric aircraft [18] and tramway systems [19], there is a lack of critical review and comparison between hybrid vehicle EMSs.

One promising way of managing power share between power sources is using fuzzy logic control (FLC). FLC is a rule-based strategy that uses fuzzy inference systems to create linguistic outputs from deterministic inputs [20]. Ahmadi et al. [21] implemented FLC into a fuel cell, battery and super-capacitor electric vehicle and benchmarked the performance against 22 different drive cycles. Multi-objective optimisation was performed using a genetic algorithm (GA) approach which resulted in performance enhancements, fuel economy improvements and better charge-sustaining capability over the non-optimised FLC. FLC has also been applied to various other vehicles, such as trams, trains and UAVs [22–24].

Equivalent consumption minimisation strategy (ECMS) is a commonly used real-time optimisation strategy in hybrid electric vehicles [25–28]. It uses an equivalent cost function that transfers the global optimisation into a local problem and is minimised at every time step [4]. It does this while maintaining the battery SOC within a specified range by the implementation of an equivalence cost factor (Eq. (17)). Cost function methodology can be used to minimise any variable, whether it is H_2 consumption or performance degradation, referred to as equivalent degradation minimisation strategy (EDMS) [29]. The implementation of a degradation minimisation EMS presents difficulties as they require complex degradation models which are highly dependent on design and materials used within the fuel cell.

Xu et al. [30] present an application of Pontryagin's Minimisation Principle (PMP) on the operating cost of a plug-in hybrid PEFC city bus. They developed an electric vehicle model using MATLAB/Simulink consisting of a fuel cell system, DC/DC converter, Li-ion battery electric motor and gearbox models. They use the platform to compare Dynamic Programming (DP), PMP, Charge Depleting Charge Sustaining (CDCS) and several blended EMSs. Each EMS was compared to one another using the operating cost, which was influenced by change in SOC and cost of hydrogen. They found the operating cost can be reduced by 7.2% by using the DP EMS compared to CDCS EMS, and by 5.9% using the PMP strategy. No notice was paid to the effects each EMS would have on wider system considerations such as degradation and system lifetime.

Li et al. [26] developed a novel ECMS using sequential quadratic programming, named SECMS, for a hybrid fuel cell, battery and supercapacitor electric vehicle. A rule-based strategy (RBS) and a hybrid ECMS-operating mode control strategy (HEOS) were used to compare the SECMS. They found their SECMS resulted in a 2.16% drop in hydrogen consumption compared to RBS and 1.47% compared to HEOS. They also note the SECMS would result in reduced degradation due to a smoother fuel cell current; however, this was not modelled or quantified.

Chen et al. [31] developed FLC so that the fuzzy parameters are tuned in real-time depending on the driving conditions of the hybrid fuel cell and battery electric vehicle. They named this approach adaptive fuzzy logic parameter tuning (AFLPT). Depending on various parameters, the fuzzy rule base can either be in three states, normal driving condition, regenerative braking condition or overload driving condition. They report AFLPT results in less deviation from the desired battery voltage compared to no AFLPT.

Yue et al. [20] developed a 'health-conscious' EMS for a fuel cell hybrid electric vehicle. Their EMS was based on a prognosis decision-making process and focused on prolonging the lifetime of the fuel cell stack. Five fuzzy logic controllers were optimised off-line using GA at different fuel cell and battery degradation states. During operation, degradation factors were determined which re-defined the rules of the fuzzy logic controllers based on classification results and Dempster-Shafer data fusion. Their modelling results show that with an opportunely adjustable FLC, fuel cell lifetime can be improved by 56% compared to a baseline EMS.

Hames et al. [25] presented a hybrid fuel cell and battery light-duty electric vehicle model for the comparison of four EMSs. They compare a peaking power source strategy (PPSS), operating mode control strategy (OMCS), fuzzy logic control (FLC) and ECMS. Comparison metrics are limited to hydrogen consumption only, with efficiency and degradation factors of the system neglected. They found the ECMS used the least H_2 during the urban dynamic driving strategy (UDDS), and FLC to use the most.

Wang et al. [32] developed a power management system for a fuel cell/battery hybrid electric vehicle with an objective function to minimise the overall lifetime cost of the system, by minimising fuel consumption and maximising the power source lifetime. Their model includes a complex fuel cell degradation model, encompassing an electrochemical surface

Please cite this article as: Luca R et al., Comparative study of energy management systems for a hybrid fuel cell electric vehicle - A novel mutative fuzzy logic controller to prolong fuel cell lifetime, International Journal of Hydrogen Energy, https://doi.org/10.1016/j.ijhydene.2022.05.192

area (ECSA) loss model coupled to operational conditions such as idle and high power. A semi-empirical capacity loss model was also used to model battery degradation. They show how varying the fuel cell cost factor (the amount the optimisation tries to minimise degradation) impacts the performance of the fuel cell and battery over time. They found minimising the fuel cell degradation increased battery degradation. It remains to be shown how this compares to other commonly used EMSs.

Physical systems

Many of these modelled EMSs have been applied to physical systems [9,33–35]. Garcia et al. [36] developed a three-way hybrid system using a fuel cell, battery and supercapacitor for a tram. They used the SC to meet peak power as it has the fastest response time, which is beyond that of the fuel cell and battery. They modelled the system in MATLAB-Simulink, using commercially available components. Their EMS used an equivalent consumption minimisation strategy to optimise hydrogen consumption. They tested their system with driving cycles for the tramway. It was found that by maintaining the DC bus voltage at 750 V the SOC of the battery and SC are best kept at 65% and 75%, respectively. They report a fuel cell efficiency of 60.9% and an overall hybrid vehicle efficiency of 55.6%.

Yufit and Brandon [37] developed a hybrid test system using off-the-shelf components including a PEFC, Li-ion battery and a DC/DC converter. They developed their system to be suitable for an unmanned underwater vehicle application and built a control algorithm to regulate the power share between the fuel cell and the battery, along with a graphical interface to visualise and record thermal and electrochemical performances. Their control algorithm was a simple flow chart that was dependent on the state-of-charge of the battery, voltage and various system temperatures. During dynamic tests, they report there was significant heat generated which resulted in the battery needing sufficient time to cool down before being able to use peak power again. This indicates a need to integrate thermal modelling considerations into an EMS design.

Summary and impact

Following a survey of current research, there remains a need to compare EMSs for electric fuel cell/battery hybrids using a common modelling framework, focusing on key factors such as power system degradation and hydrogen consumption. This paper aims to present a common modelling framework in MATLAB/Simulink, named EV-SimKit (Electric Vehicle Simulation tool-kit), and demonstrate its abilities by using it to compare EMSs for automotive applications. Finally, a novel fuzzy logic controller is presented and is demonstrated to increase fuel cell lifetime by mutating the output membership functions depending on the state-of-degradation (SoD) of the fuel cell system, appropriately named the 'mutative fuzzy logic controller' (MFLC). This significant development in fuzzy logic combines what was previously achieved only with multiple separate controllers, reducing computational cost on board the vehicle and extending the lifetime at the same time. The MFLC also extends beyond fuel cell control and is applicable to any scenario where output signals need to be adjusted based on input signals.

Models and parameterisation

This section presents the development of the electric vehicle model, semi-empirical dynamic fuel cell model and an ECM developed in MATLAB/Simulink. The fuel cell and battery models include degradation subsections.

Vehicle model

The vehicle and motor components of the model function under the basic operating principles presented in [38]. The vehicle model evaluates basic forces acting on the body, taking into account various losses such as rolling and air resistance to determine the acceleration of the vehicle, Eq. (1). Tractive power is determined from the product of tractive force and vehicle speed.

$$a = \frac{F_{tr} - (F_{rr} + F_{air} + F_{gr})}{m}. \quad (1)$$

The drive cycle input, from the Drive Cycle Source block in Simulink, is evaluated against the vehicle speed and the difference is input to a PID controller to determine the accelerator and brake pedal position. The pedal positions are input to a simple motor model which determines motor power to meet the required wheel torque to satisfy the vehicle acceleration. The required motor power is a summation of power required to move the vehicle and the power losses associated with the motor, which is expressed in Eq. (2).

$$P_{loss} = k_c\tau^2 + k_i\omega + k_\omega\omega^3 \quad (2)$$

where τ = motor torque, ω = motor speed, k_c = copper losses, k_i = iron losses, k_ω = windage losses and C = motor constant losses [38]. The motor model also accounted for energy regeneration during braking. With a regen fraction of 0.2, this is representative of the amount of energy available for regeneration in a typical electric vehicle [39]. All vehicle level and motor parameters can be found in Table 1 in the

Table 1 – Fuel cell model parameters.

Name	Value	Unit	Citation
Area	100	cm^2	–
Electrode catalyst specific area	600	$cm^2\ mg^{-1}$	–
Electrode charge transfer coefficient	0.5	–	[47,48]
Electrode activation energy	21000	$J\ mol^{-1}$	[49]
Electrode thickness	0.002	cm	[50]
Electrode catalyst loading	0.4	$mg\ cm^{-2}$	–
Electrode catalyst layer porosity	0.653	–	[50]
Anode reference exchange current density	0.0889	$A\ cm^{-2}$	
Cathode reference exchange current density	1.8395e-6	$A\ cm^{-2}$	
Electrode tortuosity	1.82	–	[50]
Membrane density	2	$g\ cm^{-3}$	–
Membrane equivalent weight	1100	$g\ mol^{-1}$	[51]
Membrane thickness (wet)	0.004	cm	[47]
Number of cells	300	–	–

Please cite this article as: Luca R et al., Comparative study of energy management systems for a hybrid fuel cell electric vehicle - A novel mutative fuzzy logic controller to prolong fuel cell lifetime, International Journal of Hydrogen Energy, https://doi.org/10.1016/j.ijhydene.2022.05.192

supplementary material. The total power demand of the vehicle is calculated using the following

$$P_{demand} = P_{mot} + P_{BoP} + P_{accessory} \quad (3)$$

Where

$$P_{mot} = \tau_{mot} \times \omega_{mot} + P_{loss}. \quad (4)$$

$P_{accessory}$ accounts for cabin electronics and P_{BoP} accounts for the FC balance-of-plant (BoP). Parameters τ_{mot} and ω_{mot} represent the motor torque and speed, respectively. The parasitic fuel cell power, or BoP power, is the sum of the compressor power, air blower power and coolant pump power. It is reported that the compressor power can be up to 93.5% of the total parasitic power [40]. Therefore, this was modelled in detail and the others were set to constant values, as in [26]. The power consumption by the compressor for a given pressure ratio and the flow rate is given by Eq. (11).

$$P_{cp} = C_p \frac{T_{atm}}{\eta_{cp}} \left[\left(\frac{P_{out}}{P_{in}} \right)^{\frac{\gamma-1}{\gamma}} - 1 \right] \dot{m}. \quad (11)$$

where C_p is the specific heat capacity of air, T_{atm} is the atmospheric temperature, η_{cp} is the compressor efficiency, P_{out} is the pressure out of the compressor (FC pressure), P_{in} is the pressure into the compressor (atmospheric pressure), γ is the ratio of specific heats of air and $\dot{m}$ is the mass flow rate of air required by the fuel cell.

Equivalent circuit model

An equivalent circuit model (ECM) uses electrical circuit components to mimic the voltage response of a battery [41]. Its semi-empirical nature ensures high versatility and low computational load when modelling whole battery packs. Fig. 2 shows the pulse discharge for a single temperature, ECM design and parameterisation.

The ECM was parameterised to a Samsung 20R 18650 by pulse discharging at four temperatures, 10, 20, 30 and 40 °C. Parameterisation was performed using the Estimation Equivalent Circuit Battery block and experimental data acquired using a Maccor 4200 battery cycler with MTC-020 environmental chambers (USA). The code for the parameter extraction was originally presented in [42], which is now included in the Powertrain Blockset in MATLAB/Simulink. The mean residual was 2.99 mV along the entire discharge curve. The values for the resistors and capacitors as a function of state-of-charge (SOC) and temperature can be seen in Supplementary Material Fig. 1. To isolate the effects of the electrical EMS, the temperature of the battery pack was assumed to be a constant 313 K during the simulations.

The ECM was integrated into the hybrid vehicle model using the in-built Simulink Equivalent Circuit Battery block. The current and voltage was multiplied by the number of cells in parallel and series respectively to build the battery pack.

Battery degradation model

The semi-empirical battery degradation model is based on experimental data from the same cell used to characterise the ECM. The degradation is based on an increase in cell internal resistance and capacity loss, as a result of charge throughput. Fig. 3a shows the capacity loss over 350 cycles, and Fig. 3b shows the increase in internal resistance over the same number of cycles.

Cycling the cell 350 times resulted in an increase in the internal resistance of 2.58 mΩ, or an average increase of 7.37×10^{-5} Ω per cycle. This was determined from the change in real resistance at the inflection point, which is typically used by battery management systems (BMS) to determine internal resistance [43]. A cycle was defined as one charge and discharge, an average of 3848 mAh. The total capacity loss was 84 mAh, equivalent to 0.24 mAh per cycle. The semi-empirical part was adjusted from the work by [44,45], where acceleration factors based on current, temperature and DOD increased the degradation rate. The full degradation model can be seen in Eqs. (5) and (6).

$$R_{increase} = R_0 N \left(\frac{I}{I_{ref}} \right) \exp\left(\frac{1}{T} - \frac{1}{T_{ref}} \right) \left(\frac{0.5}{DOD} \right) \quad (5)$$

$$C_{loss} = C_0 N \left(\frac{I}{I_{ref}} \right) \exp\left(\frac{1}{T} - \frac{1}{T_{ref}} \right) \left(\frac{0.5}{DOD} \right) \quad (6)$$

where R_0 and C_0 are the parameterised degradation rates, N is the number of cycles, I is the cell current, T is the cell temperature, DOD is the depth-of-discharge and I_{ref} and T_{ref} are the reference parameters which were based on the conditions of cycling in Fig. 3.

Fuel cell model

A one-dimensional, dynamic PEFC model was implemented into the model using a MATLAB function block and open-source code developed by Lazar et al. [46]. The model calculates the cell voltage by subtraction of activation, ohmic and mass transport overpotentials at every operating current. The model reduced computational load by excluding MEA composition and treating it as a black box. This allows the model to be implemented into a more complex model, such as a vehicle model and real-time applications. However, the model does incorporate water transport through the membrane by the means of osmosis, diffusion and hydraulic permeation.

The model was parameterised to a HyPlat GDE (HyPlat Ltd, Cape Town, SA) and a Gore −Select (Gore & Associates, Newark, USA) membrane. Parameters can be seen in Table 1.

Fig. 4a shows a polarisation curve from the fuel cell model parameterised against experimental data. Data was acquired using a Greenlight testing station on a single 100 cm^2 metallic fuel cell with serpentine flow field geometry with HyPlat and Gore MEAs. The fitting was performed by adjusting voltage correction coefficients and exchange current densities. The calculated cell voltage was multiplied by the number of cells in the stack to obtain the total stack voltage.

The fuel cell system efficiency is a combination of several efficiencies associated with the fuel cell [53]. First is the reversible efficiency:

$$\eta_{rev} = \frac{\Delta G_f}{\Delta H_f} \quad (7)$$

Please cite this article as: Luca R et al., Comparative study of energy management systems for a hybrid fuel cell electric vehicle - A novel mutative fuzzy logic controller to prolong fuel cell lifetime, International Journal of Hydrogen Energy, https://doi.org/10.1016/j.ijhydene.2022.05.192

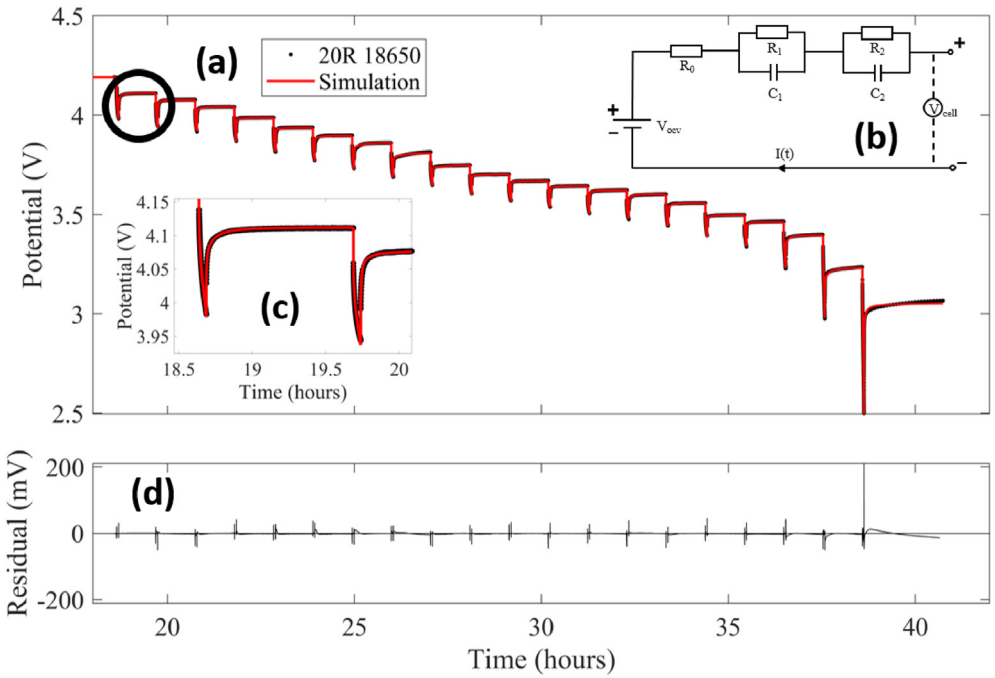

Fig. 2 – Pulse discharge of 18650 (black) and ECM simulating the pulse discharge (red). The voltage residual plot can be seen in the bottom plot (d) with a mean residual of 2.99 mV. Top right inset (b) shows the equivalent circuit used to model the cell, which consists of a series resistor, two resistor-capacitor pairs and the open-circuit source. The bottom left inset (c) shows a close-up of the voltage response to a current pulse. Pulse magnitude was 2 A (1C) with a duration of 3 min, resulting in 20 characterisation points. (For interpretation of the references to colour in this figure legend, the reader is referred to the Web version of this article.)

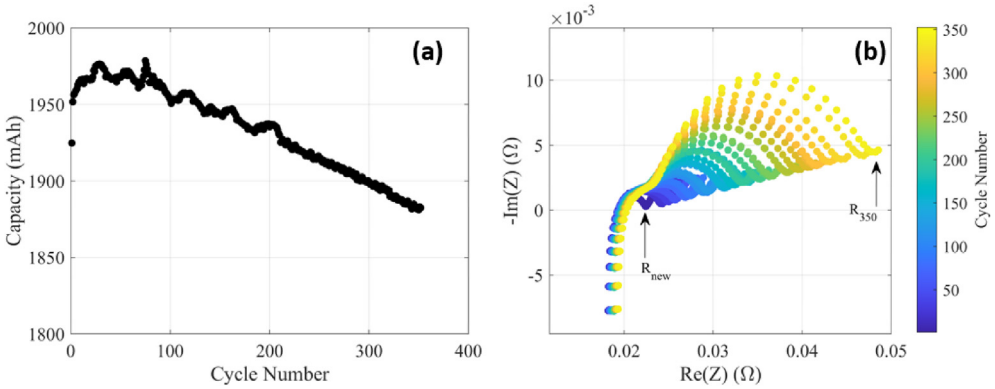

Fig. 3 – Capacity fade plot (a) and Nyquist plot (b) for a commercial Samsung 20R cycling at 2C with no constant voltage (CV) stage at ambient temperature.

where ΔG_f is the Gibbs free energy of formation, and ΔH_f is the enthalpy of formation. The second is the voltage efficiency:

$$\eta_{vol} = \frac{E}{E_{rev}}. \tag{8}$$

where E is the cell voltage, and E_{rev} is the reversible cell voltage. Next, there is the fuel utilisation efficiency, μ_{fuel}, which is the fraction of fuel consumed in the cell. We then have the power conditioning efficiency, μ_{pc}, and then parasitic efficiency, η_p, which accounts for the BoP:

$$\eta_p = 1 - a - \frac{b}{Ei}. \tag{9}$$

where a and b are empirical constants. Here, it is assumed $\mu_{fuel} = 0.95$, $\mu_{pc} = 0.95$, and a and b are equal to 0.0499 and 0.05 respectively [53]. The high fuel utilisation efficiency was assumed due to an on-board hydrogen recirculation system. The fuel cell system efficiency is then the product of all constituent efficiencies:

Please cite this article as: Luca R et al., Comparative study of energy management systems for a hybrid fuel cell electric vehicle - A novel mutative fuzzy logic controller to prolong fuel cell lifetime, International Journal of Hydrogen Energy, https://doi.org/10.1016/j.ijhydene.2022.05.192

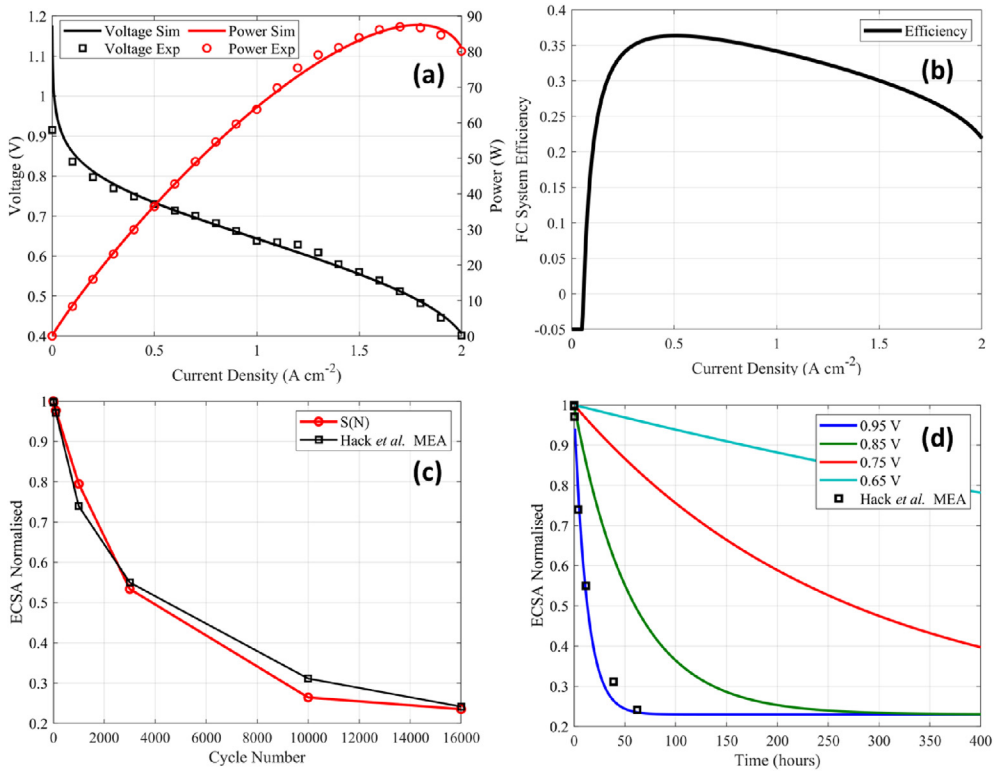

Fig. 4 – Fuel cell polarisation curve from experiment and parameterised model (a), fuel cell system efficiency against current density (b), electrochemical surface area loss model parameterised with data obtained from [52] (c) and effect of upper potential limit on electrochemical surface area loss (d).

$$\eta_{sys} = \frac{nFE}{\Delta H_f}\left(\mu_{fuel}\mu_{pc}\right)\left(1 - a - \frac{b}{Ei}\right). \tag{10}$$

System efficiency against power output can be seen in Fig. 4b. At very low stack powers, the system efficiency becomes negative due to constant BoP parasitic power consumption to maintain OCV, hence the efficiency is set to −0.05 under these conditions.

The temperature of the FC stack was set to a constant 333 K throughout the simulations. This was done to isolate the effect of the EMS on system performance, as the thermal management system will also impact degradation rates and system efficiency.

Fuel cell degradation model

The fuel cell degradation model is comprised of an electrochemical surface area (ECSA) loss model coupled with operational conditions, which are known to cause accelerated degradation. This approach has been previously demonstrated in [32]. The ECSA loss model was adapted from [54], which models the ECSA decay rate as a function of the remaining Pt surface area:

$$\frac{dS}{dN} = -k\,S(N). \tag{12}$$

where $\frac{dS}{dN}$ is the Pt surface area decay rate, k the decay rate constant and $S(N)$ is the Pt surface area. It has been shown that Pt surface area tends to a minimum value, where further loss becomes increasingly unlikely. This value has been determined to be approximately 20% of the original value [55,56]. Therefore, ECSA loss can be represented by the following exponential decay function

$$S(N) = S_{min} + (1 + S_{min})e^{(-kN)} \tag{13}$$

which is obtained by integrating Eq. (12) between $1 - S_{min}$ and $S(N) - S_{min}$. N represents the cycle number of the accelerated stress test (AST). The decay constant depends on several factors, such as temperature, humidity and voltage. Parameterising this model to the ECSA loss data presented in Fig. 4c gave a k_{AST} value of 3.1031×10^{-4}. Data were obtained in a previous study by Hack et al. [52]. The upper voltage of the AST was 0.95 V, which is not always the operating condition of the fuel cell. Therefore, the k value can be modified using Eq. (14).

$$k = k_{AST}\, e^{C(UPL - UPL_{AST})} \tag{14}$$

where, UPL is the upper potential limit of the fuel cell and UPL_{AST} is the upper potential limit of the AST, and C is a constant set to 0.0152 mV^{-1} [54].

Pei et al. [57] break down the degradation of a fuel cell into four key operating regions: load change; stop/start; idle and high power, indicated by $P_1 - P_4$ in Eq. (15), respectively.

$$T_f = \frac{\Delta P}{k_p(P_1 n_1 + P_2 n_2 + P_3 t_3 + P_4 t_4)} \tag{15}$$

where ΔP is the maximum allowable performance decay, k_p is an accelerating factor set to 1.72 [57] and n_1, n_2, t_3, t_4 denote

Please cite this article as: Luca R et al., Comparative study of energy management systems for a hybrid fuel cell electric vehicle - A novel mutative fuzzy logic controller to prolong fuel cell lifetime, International Journal of Hydrogen Energy, https://doi.org/10.1016/j.ijhydene.2022.05.192

the number of load changes and stop/start occurrences, and the time of idle and high power respectively. The approach to convert $P_1 - P_4$ to the equivalent ECSA loss values was followed from [32] and resulted in the following: $P_1 = 0.002199$ %/load change, $P_2 = 4.54 \times 10^{-5}$ %/stop/start cycle, $P_3 = 0.0545$ %/hour and $P_4 = 0.0467$ %/hour. The only caveat is the AST clearly degrades the FC significantly faster compared to normal operation. It is predicted that an AST lasting 200 h is equivalent to the same as three years of degradation under normal conditions [58,59]. Therefore, a factor of 100 was removed from the decay rates to account for this, already included in the values above.

Energy management system

The EMS manages the share of total power demand between the fuel cell stack and the battery pack. Depending on various system parameters such as SOC, temperature and load type, the power drawn from each power source will vary. Five EMS were built into the Simulink workspace, as seen in Fig. 5, and are detailed in the following subsections.

Rate Limited Power

A simple Rate Limited Power (RLP) EMS was used as a baseline. The inputs to this EMS was the power demand and battery SOC. The FC power followed the power demand but a rate limiter was used to ensure there were no large step changes in FC power. The rate limiter prevented the FC from increasing and decreasing faster than a rate of 0.4% of total power per second. The battery power was set to the difference between the power demand and FC power output. If the battery SOC was greater than 60%, the fuel cell power ramped down to maintain the SOC in the optimal range and prevent excessive fuel usage. Fig. 5b shows this control system implemented

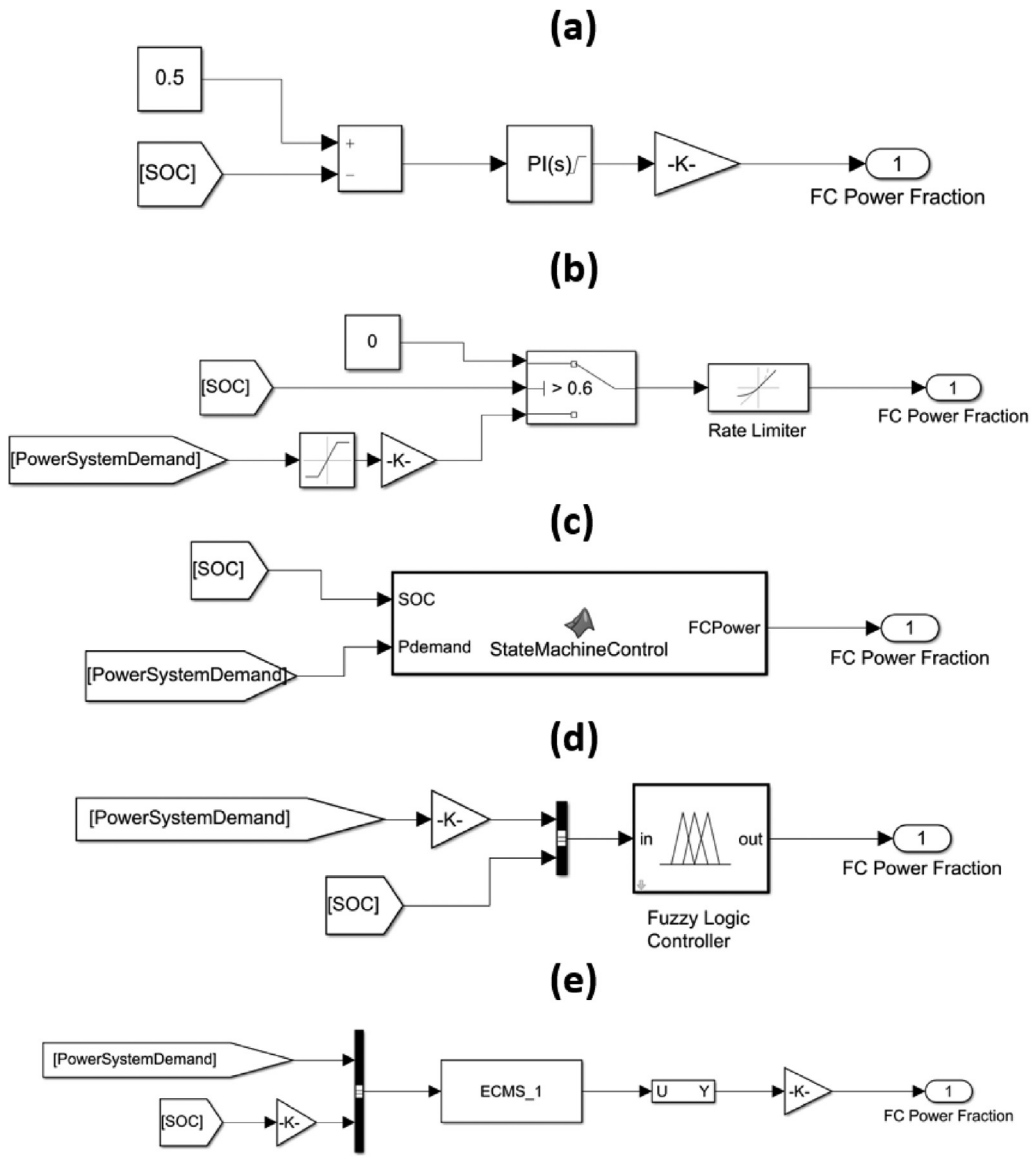

Fig. 5 – Implementation of EMSs in Simulink workspace in the following order: PI Control, Rate Limited Power, State Machine Control, Fuzzy Logic Control and Equivalent Consumption Minimisation Strategy.

Please cite this article as: Luca R et al., Comparative study of energy management systems for a hybrid fuel cell electric vehicle - A novel mutative fuzzy logic controller to prolong fuel cell lifetime, International Journal of Hydrogen Energy, https://doi.org/10.1016/j.ijhydene.2022.05.192

into the Simulink workspace. The output is a value between 0 and 1 which represented the fraction of maximum fuel cell power. The maximum FC power was set to the power output at 1.25 A cm^{-2}, or approximately 0.6 V per cell.

Conventional fuzzy logic control

Fuzzy logic control (FLC) calculates continuous output values based on a set of predefined rules, membership functions (MF) and imprecise inputs [21]. These predefined rules are based on user knowledge which makes the control of fuzzy logic sub-optimal. This can be improved with the use of an optimisation method to tune the membership functions. For this work, a basic FLC was implemented and optimised using a gradient descent method with a sequential quadratic programming algorithm in Simulink Design Optimisation.

The FLC had two inputs, power demand and SOC, and a single FC power fraction output. The user knowledge base is inputted in the form of a set of rules. A rule-base is used to inform the FLC what the output should be depending on a set of input conditions. For example; "if SOC is high" and "power demand is low" then "FC output is low" is a single rule. All rules used in the system can be seen in Table 2.

The optimisation aims were to minimise the degradation cost by adjusting the output membership function parameters while ensuring the battery SOC did not fall below 45% from a starting value of 50%. The degradation cost, D_{cost}, is quantified using Eq. (16):

$$D_{cost} = \alpha(C_{fc} \cdot D_{fc}) + \beta(C_b \cdot D_b) \tag{16}$$

where C_{fc} is the cost of the fuel cell system, set to DoE 2020 target of \$30/kW, D_{fc} is the degradation of the fuel cell system, C_b is the cost of the battery pack, set to the DoE 2020 target of \$125/kWh and D_b is the degradation of the battery pack. Pack end-of-life (EoL) was taken to be 80% of beginning-of-life (BoL) capacity. As each cell has a capacity of 2 Ah, pack degradation was calculated using:

$$D_b = \frac{C_{loss}[mAh]}{400}. \tag{17}$$

The fuel cell degradation, D_{fc}, was determined from the ECSA percentage loss over the EoL condition, set to 27% remaining ECSA. Degradation constants, α and β, can be used to make the equivalent cost comparable; however, they were both set to one during this optimisation. This quantity is also used to compare each EMS in Results and Discussion.

All input and output membership functions were of a Gaussian type to allow ease of control during optimisation. Fig. 6c and d shows the output membership function before and after optimisation, which resulted in a reduction of \$3.00 over the duration of the drive cycle, as can be seen in Fig. 7b. The majority of this cost-saving came from a reduction in degradation due to load change by increasing the width of the medium MF and reducing the step size to the high and low MFs. This is discussed further in Results and Discussion.

Fig. 7c and d shows the fuzzy surfaces, where the output (FC power fraction) is displayed on the z-axis with each input on the x- and y-axis. The changes due to the optimisation can be clearly seen, with the peak and average FC power decreasing and the creation of a plateau where the fuel cell will operate the majority of the time.

The FLC was implemented into the Simulink model using the Fuzzy Logic Controller bock which links to the fuzzy inference system (FIS) in the MATLAB workspace. The block diagram can be seen in Fig. 5d.

Table 2 – Rules of FLC. L = low, M = medium, H = high, P = positive, N = negative.

FC Power		Power Demand					
		NH	NM	NL	PL	PM	PH
SOC	L	L	L	H	H	H	H
	M	L	L	L	M	M	H
	H	L	L	L	L	L	M

Mutative fuzzy logic controller

The optimised FLC was developed further by introducing fuel cell degradation as a third input. This was quantified as 'state-of-degradation' (SoD) with 0 being the beginning-of-life and 1 the end-of-life condition. Moving the degradation between a state of low to medium, according to the membership functions seen in Fig. 6e, triggers a mutation of the output membership functions, hence the name mutative fuzzy logic controller (MFLC), with the goal to prolong fuel cell lifetime. These mutations follow the general trend of reducing the average fuel cell power output and decreasing its dynamic response to load changes. The output membership functions of the MFLC can be seen in Fig. 6f. Three levels of fuel cell degradation were used in this example, low degradation which corresponds to an SoD between 0 and 0.3, medium degradation which corresponds to 0.2–0.8 and high which corresponds to an SoD of 0.7–1. The effect of the MFLC on fuel cell lifetime will be discussed in Results and Discussion.

Equivalent consumption minimisation strategy

The ECMS is based around the implementation of a cost function that minimises the fuel usage of the system [18]. It does this within pre-defined operating regimes of battery power, SOC and FC power. The cost functions aim to minimise Eq. (18):

$$F = (P_{fc} + \alpha P_{batt})dt \tag{18}$$

where α is the equivalence factor expressed by Eq. (19).

$$\alpha = 1 - 2\mu\frac{(SOC - 0.5(SOC_{min} + SOC_{max}))}{SOC_{min} + SOC_{max}} \tag{19}$$

where μ is the SOC balance coefficient, typically 0.6, SOC_{min} is the minimum SOC level of the battery pack and SOC_{max} is the maximum SOC of the pack. The equality constraint, Eq. (20), ensures the power demand is always met.

$$P_{demand} = P_{fc} + P_{batt}. \tag{20}$$

The following boundary conditions apply to ensure the FC power, SOC and battery power are all operating within their limits (21)–(23).

Please cite this article as: Luca R et al., Comparative study of energy management systems for a hybrid fuel cell electric vehicle - A novel mutative fuzzy logic controller to prolong fuel cell lifetime, International Journal of Hydrogen Energy, https://doi.org/10.1016/j.ijhydene.2022.05.192

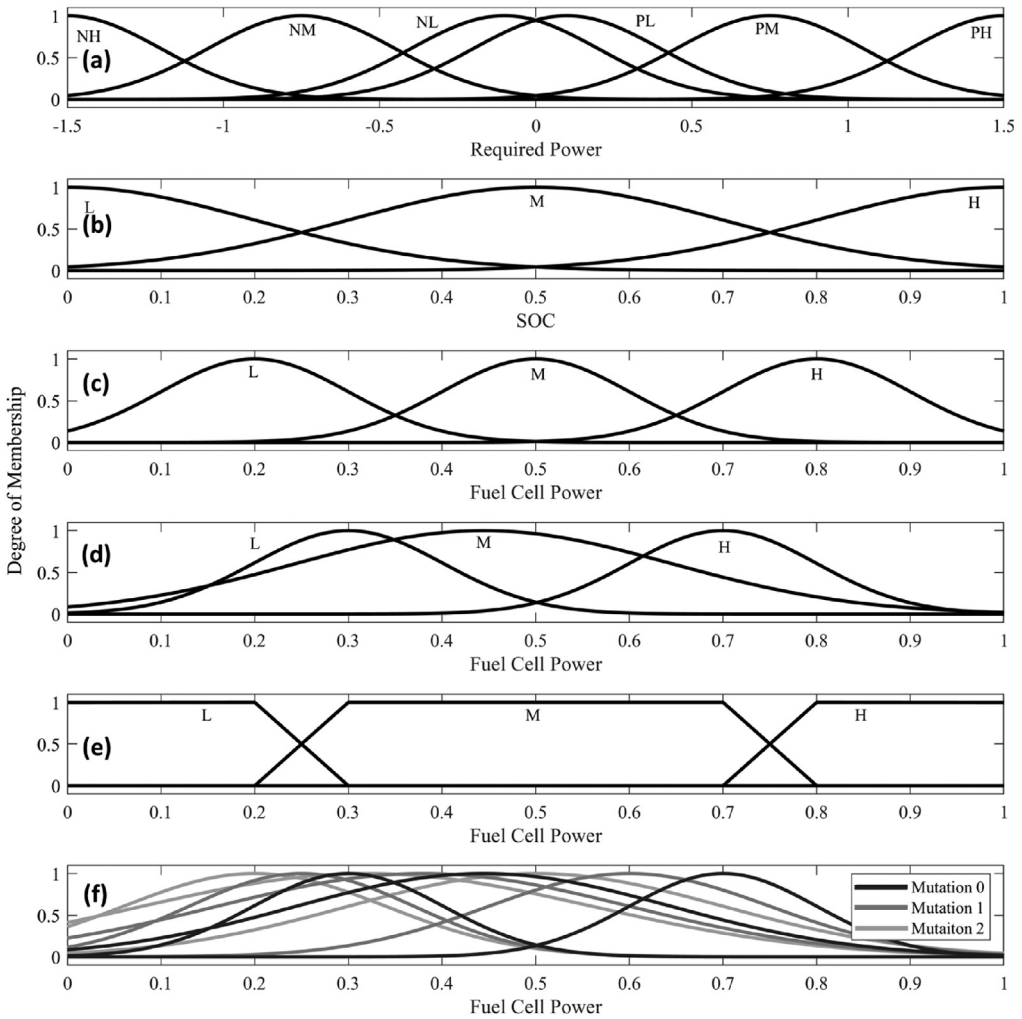

Fig. 6 – FLC membership functions, with power demand input (a), SOC input (b), FC power fraction non-optimised (c), FC power fraction optimised (d), MFLC FC degradation input (e) and MFLC FC power fraction outputs (f). L = low, M = medium, H = high, P = positive, N = negative.

$$P_{fc,\,min} \leq P_{fc} \leq P_{fc,max}. \quad (21)$$

$$P_{batt,min} \leq P_{batt} \leq P_{batt,max}. \quad (22)$$

$$1.4 \leq \alpha \leq 1.8. \quad (23)$$

The cost function was implemented into the Simulink workspace using a MATLAB S-Function block (Fig. 5e). The MATLAB function *fmincon* minimised the cost function every step during the computation.

Classic PI control

A proportional-integral (PI) control was set to maintain the battery SOC around a fixed value; in this case, it was 50%. The error in SOC to the ideal value was used to determine the FC power.

State machine control

The implemented state machine control (SMC) is based on the EMS in Ref [18,22]. Each state is defined by two inputs, with a fixed output for each state. These are presented in Table 3. This control logic was implemented with a MATLAB function block, where *If statements* were used to segment the states.

Results and Discussion

The Worldwide Harmonised Light Vehicle Test Protocol (WLTP) (Class 3) was used to simulate the vehicle driving conditions [60]. This drive cycle was chosen as it consists of four characteristic driving scenarios; urban; suburban; rural and highway driving, each with a different maximum speed, which can be seen in Fig. 8a. Each test case had the same initial conditions to allow for comparison. Fig. 8 shows

Please cite this article as: Luca R et al., Comparative study of energy management systems for a hybrid fuel cell electric vehicle - A novel mutative fuzzy logic controller to prolong fuel cell lifetime, International Journal of Hydrogen Energy, https://doi.org/10.1016/j.ijhydene.2022.05.192

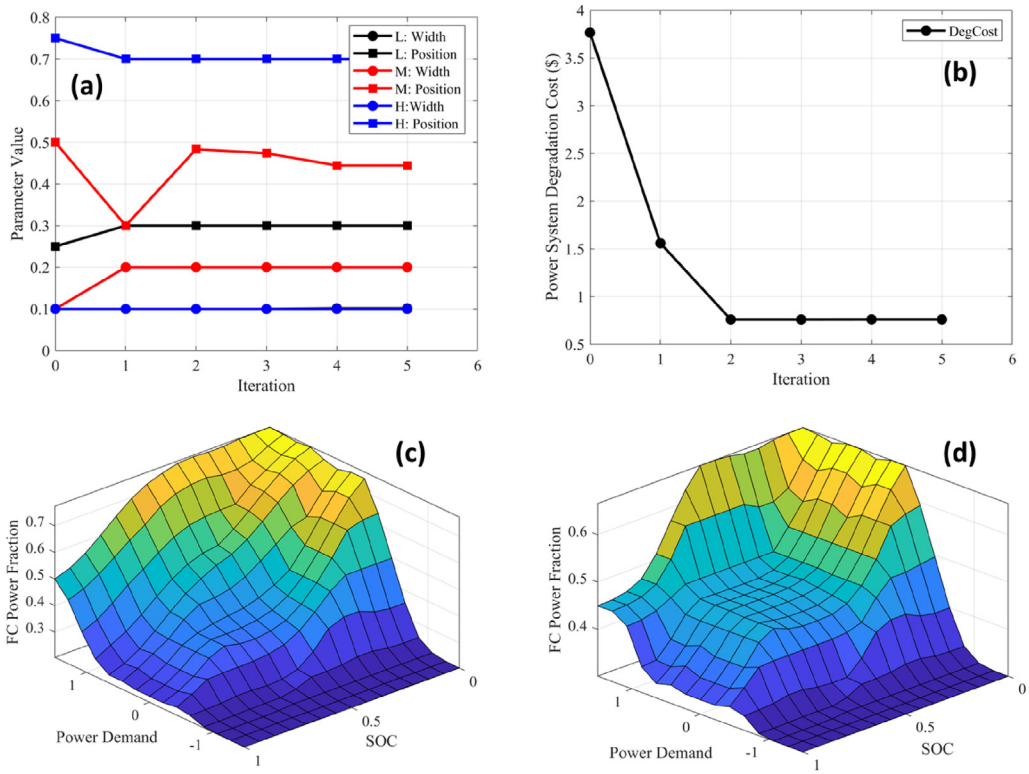

Fig. 7 – Output membership function parameters and cost during optimisation, (a) and (b) respectively, non-optimised FC power surface (c) and optimised FC power surface (d).

Table 3 – State Machine Control States [18]. $P_{fc\ min}$ = minimum FC power, $P_{fc\ max}$ = maximum FC power, P_d = power demand, $P_{fc\ opt}$ = optimal FC power and P_{chg} = battery charge power.

State	SOC	Demand Power (P_d)	Fuel Cell Power
1	High	$P_d < P_{fc\ min}$	$P_{fc\ min}$
2	High	$P_{fc\ min} < P_d < P_{fc\ max}$	P_d
3	High	$P_d > P_{fc\ max}$	$P_{fc\ max}$
4	Normal	$P_d < P_{fc\ opt}$	$P_{fc\ opt}$
5	Normal	$P_{fc\ opt} < P_d < P_{fc\ max}$	P_d
6	Normal	$P_d > P_{fc\ max}$	$P_{fc\ max}$
7	Low	$P_d < P_{fc\ max}$	$P_d + P_{chg}$
8	Low	$P_d > P_{fc\ max}$	$P_{fc\ max}$

example plots of the simulation using the PI EMS. Fig. 8a shows the drive cycle and the vehicle speed, which are seen to be identical. The motor was assumed to be able to apply sufficient torque to meet these criteria. It was also assumed the power systems were able to meet the demand of the motor instantaneously.

Fig. 8b shows the drive cycle transformed into a tractive power cycle and motor input power using the equations in Section Vehicle model. The motor input power is higher than the tractive power due to the motor losses defined in Eq. (2). Negative tractive power is a result of the vehicle decelerating. A negative motor input power represents a period of regenerative braking when the motor is acting as a generator. Peak regenerative power is significantly lower than tractive power due to the regen fraction, a variable that is adjustable in modern electric vehicles. The difference between regen power and negative tractive power is provided by the friction brakes.

Fig. 8c shows the power split between the fuel cell and battery pack under a PI controlled EMS. The inputs to the PI EMS were power demand and battery SOC. As the SOC deviated away from the ideal value (set to 0.5 in these simulations), the FC power fraction increased to bring the SOC back to ideal levels. This can be seen between 0 and 600 s. As the vehicle began to move, the SOC quickly dropped below 0.5, therefore the FC power began to increase. As the vehicle came to a significant rest around 400 s, excess FC power went back into the battery pack and therefore the SOC increased. When the SOC passed 0.5, the FC power began to ramp down to save excess H_2 consumption. During suburban driving, (500–1000 s) the SOC dropped again below 0.5 and the fuel cell power ramped up to recharge the battery pack.

Each EMS operated the vehicle power system in vastly different ways. The characteristic of each EMS can be summarised by these key attributes; average FC power; peak FC power ramp rate; peak FC power; average battery pack power; peak battery pack power; number of stop/starts; time spent at OCV.

Table 4 quantifies the results for the key attributes of each EMS. The fuzzy logic controllers and their programming for what constitutes a low or medium level of SOC resulted in a relatively high power output from the fuel cell. This resulted a negative average power for the battery pack, indicating the battery pack ended the drive cycle with a higher SOC than it started. In fact, this was the case for all but PI and RLP EMSs. It

Please cite this article as: Luca R et al., Comparative study of energy management systems for a hybrid fuel cell electric vehicle - A novel mutative fuzzy logic controller to prolong fuel cell lifetime, International Journal of Hydrogen Energy, https://doi.org/10.1016/j.ijhydene.2022.05.192

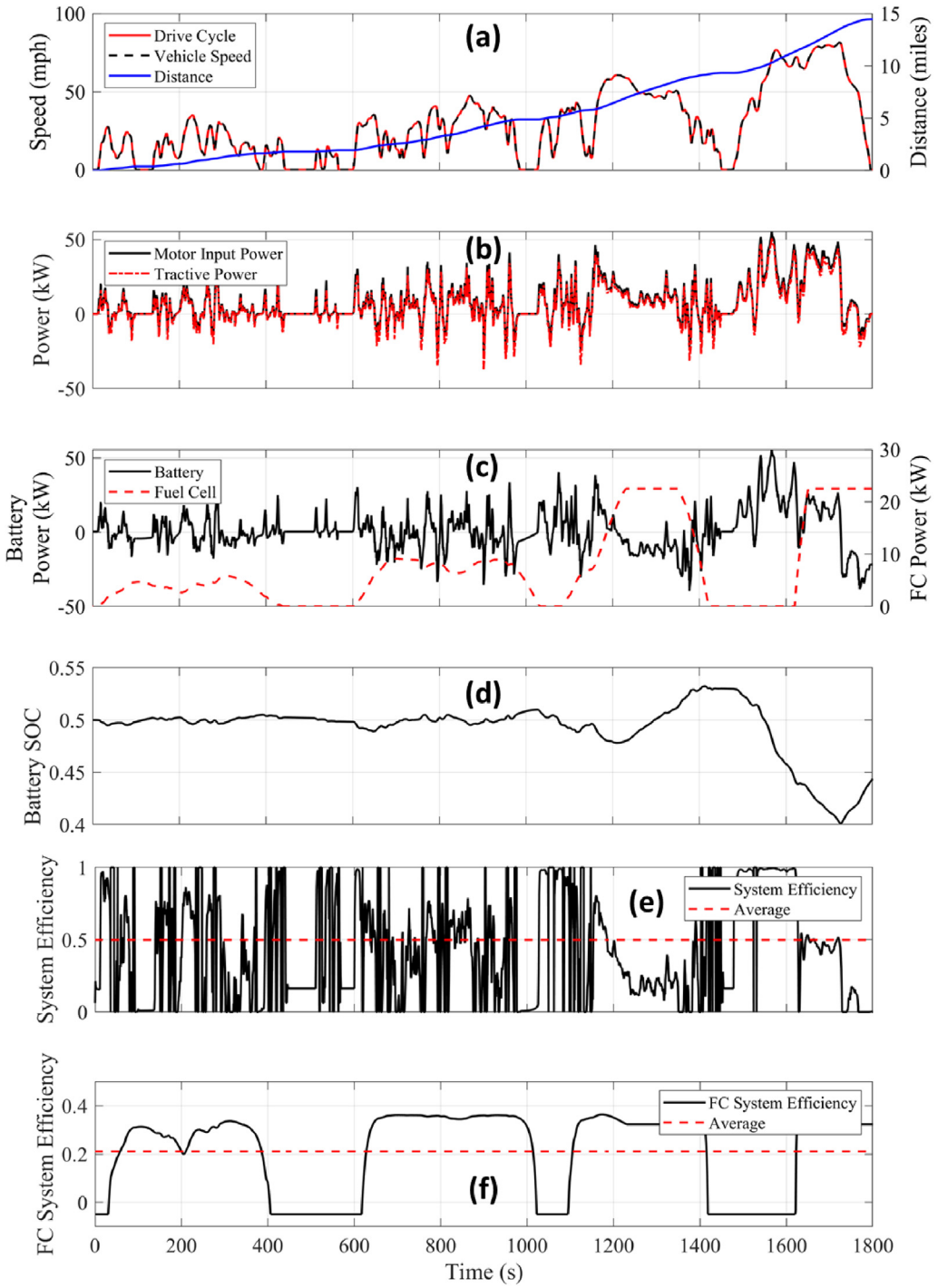

Fig. 8 – Output plots for PI-controlled system. (a) Shows the WLTP Class 3 drive cycle with vehicle speed, and the distance travelled over the drive cycle, (b) shows the required tractive power and motor input, which is slightly higher than tractive power due to motor losses, (c) shows the power output/input of the battery pack and power output of the fuel cell stack, (d) shows how the battery SoC changes throughout the drive cycle, (e) shows the total system efficiency and (f) shows the fuel cell system efficiency.

is no surprise that the average power of the battery pack was very close to zero. This is because it is designed to supply the average power requirement of the drive cycle, hence no new energy from the battery pack should be required. Due to the PI controller being backward facing, only reacting when the SOC dropped a certain level, it is effectively playing catch-up, and hence PI had the largest average draw from the battery pack. Perhaps what is more interesting is the dynamics of each EMS, which is quantified here by the peak rate-of-change of fuel cell power (P'_{fc}). Because the RLP EMS was limited to 0.4% increase

Please cite this article as: Luca R et al., Comparative study of energy management systems for a hybrid fuel cell electric vehicle - A novel mutative fuzzy logic controller to prolong fuel cell lifetime, International Journal of Hydrogen Energy, https://doi.org/10.1016/j.ijhydene.2022.05.192

Table 4 – Values for key attributes for each EMS. Meaning for column headings follow the key attribute listed above. Units for power are kW, stop starts are number of occurrences and time spent at OCV is in seconds.

EMS	$\overline{P_{fc}}$	P'_{fc}	$\widehat{P_{fc}}$	$\overline{P_{batt}}$	$\widehat{P_{batt}}$	Stop/Starts	t_{OCV}
PI	6.62	1.08	22.5	1.75	55.7	8	401
ECMS	9.41	1.79	25.5	−1.18	30.5	167	430
SMC	9.99	1.57	22.5	−1.47	33.5	1	0
RLP	8.35	0.100	17.9	0.121	48.1	1	0
FLCS	10.82	2.38	17.5	−2.24	38.4	1	0
FLCO	12.11	1.35	15.1	−3.49	42.1	1	0

in fuel cell power per second, the peak rate is therefore equivalent to 100 W per second. ECMS, SMC and FLCS all has high rates of change, which all lead to high levels of degradation. The optimisation of the fuzzy logic controller reduced the peak rate of change by 43.3% from 2.38 kW/s to 1.35 kW/s. This quantity has a severe impact on fuel cell and battery degradation, which is explored more in later sections.

In the following sections, the effect each EMS has on system and fuel cell efficiency is analysed, and then the effect each EMS has on power system degradation is quantified.

Effect of EMS on system efficiencies

The total efficiency of the vehicle power system was calculated to provide an overall comparison for efficiency. This was defined as:

$$\eta_{sys} = \frac{Useful\ Energy}{Total\ Energy} \tag{24}$$

where the useful energy was taken as the energy to power the motor, inclusive of motor losses, and total energy is the summation of energy in H_2 used and change of battery SOC. Fuel cell system efficiency calculations are detailed in Section Fuel cell model. Fig. 8e shows the total system efficiency on a point-by-point basis. The cause of the abrupt nature of the plot fluctuating across the entire range is that when the system regenerates power, the instantaneous efficiency steps to above 1. When the vehicle is at rest, the efficiency drops to below 0 as the fuel cell is still using a small amount of fuel to maintain OCV. During this period the fuel cell system efficiency was set to −0.05. The average of total system efficiency was used for comparison, which can be seen in Fig. 9a for each EMS.

As a result of the hybrid specifications chosen (25.5 kW fuel cell and 11.1 kWh pack), the total system efficiency was highly dependent on how the energy was managed between the fuel cell and battery. Note, these system sizes were specified for this study, and this paper does not constitute a sizing optimisation exercise, rather a power share strategy study. For example, if most of the energy came from the battery pack, the resulting efficiency was high. If the fuel cell provided most of the energy required, the average system efficiency was much lower due to the lower system efficiency of the fuel cell, which is approximately 35%. This resulted in a trade-off between SOC sustaining performance and system efficiency, which can be seen clearly in Fig. 9a.

Due to the positioning of the SOC membership functions in fuzzy logic controller standard (FLCS) and fuzzy logic controller optimised (FLCO), the fuel cell operated at high power for most of the test as the controller defaulted to having a high SOC level. This resulted in a high fuel cell system efficiency of over 36% but a low total system efficiency of around 26%. This was due to using H_2 to charge the battery pack, which ended the drive with a SOC of 65.0% for the FLCO EMS. It is noted that this energy will then be available next time the vehicle is used. Although total system efficiency was the lowest, the FC system efficiency was the highest. This was due to the controller operating the fuel cell at a fairly constant load of 12 kW, a result of minimising the degradation cost. The opposite of this performance was the PI EMS. This EMS operated the fuel cell at a fairly low average power, with significant time spent idling, resulting in a very low average fuel cell system efficiency of 21.1%. This also resulted in a fairly poor charge sustaining ability, but therefore a very high total system efficiency of 49.8%. Hybrid vehicles typically do not have direct grid charging of the battery pack and therefore the ability to sustain the state-of-charge is essential.

Effect of EMS on power system degradation

Choice of EMS had a significant impact on fuel cell and battery pack degradation. As detailed in Section Battery degradation model, the fuel cell degradation model captures four key operational conditions: load change, stop/start, idle and high power operation, which all accelerate fuel cell degradation. Fig. 9b shows the magnitude of these factors for each EMS (note this is plotted on a log scale). Over a single drive cycle, RLP had the lowest impact on fuel cell degradation, with a total degradation cost of $0.028 from high power operation and stop/start. However, due to the FC acting more passively, RLP EMS resulted in the second-highest battery degradation cost of $0.136. The optimised FLC performed well in terms of FC degradation with a cost of $0.65, a reduction of $4.05 compared to the standard FLC. Most of this came from lower cost due to load change, achieved by increasing the width of the output membership functions. The optimisation results in a slightly increased battery degradation due to the fuel cell acting more passively; however, this is insignificant compared to the cost reduction in fuel cell degradation.

ECMS performed the worst with a fuel cell degradation cost of $12.58, the majority coming from load change effects ($12.31). This occurred because ECMS kept increasing the fuel cell power from zero to maximum power every time there was significant demand, as it is only programmed to reduce H_2 usage. However, ECMS has the lowest battery pack degradation due to this behaviour, costing only $0.034. SMC also performed well for battery degradation due to the high average power of the fuel cell, along with large transients to meet peak power, resulting in lower peak current and less charge throughput from the battery pack.

Fig. 9d shows the total power system degradation cost for each EMS. The optimised FLC shows the best overall performance, as power system degradation cost is low and it displayed very good charge sustaining ability. It operated the fuel cell system at the highest efficiency which is the key quantity as the fuel cell provides all of the energy required for driving.

Please cite this article as: Luca R et al., Comparative study of energy management systems for a hybrid fuel cell electric vehicle - A novel mutative fuzzy logic controller to prolong fuel cell lifetime, International Journal of Hydrogen Energy, https://doi.org/10.1016/j.ijhydene.2022.05.192

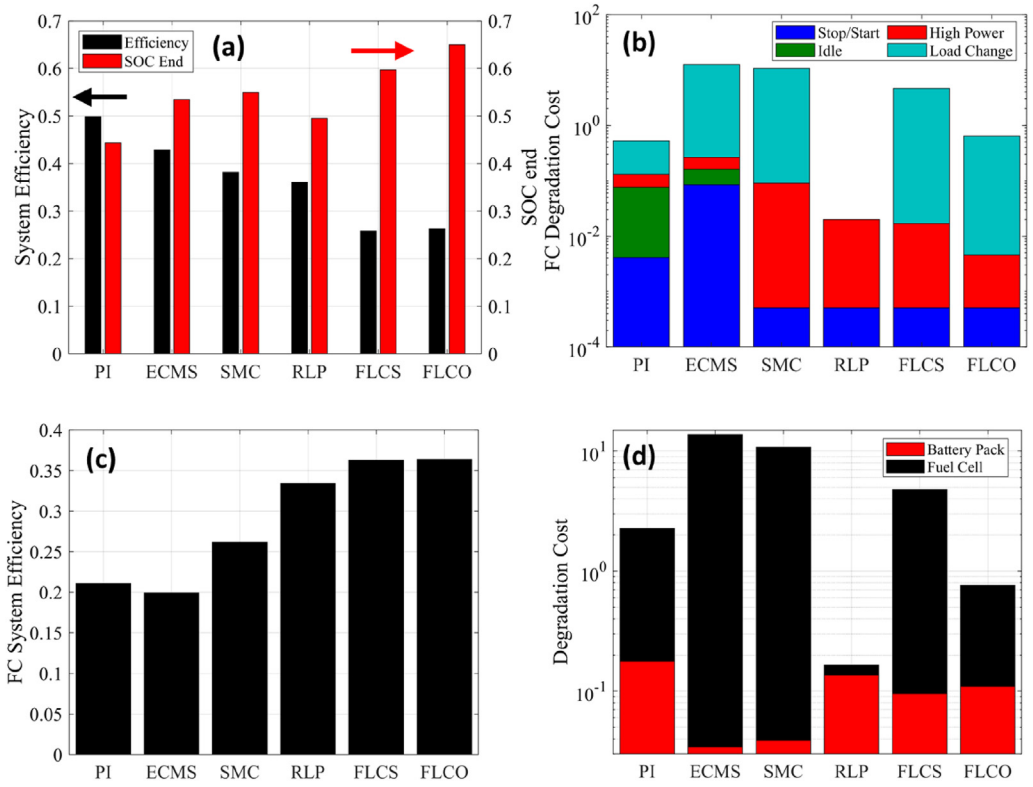

Fig. 9 – Bar chart highlighting the trade-off between system efficiency and remaining SOC (a) and comparison of FC degradation mechanism cost (b) (log scale). FC system efficiency for each EMS (c) and total degradation cost, with FC cost in black and battery cost in red (d). Plots which refer to cost are calculated in USD ($). (For interpretation of the references to colour in this figure legend, the reader is referred to the Web version of this article.)

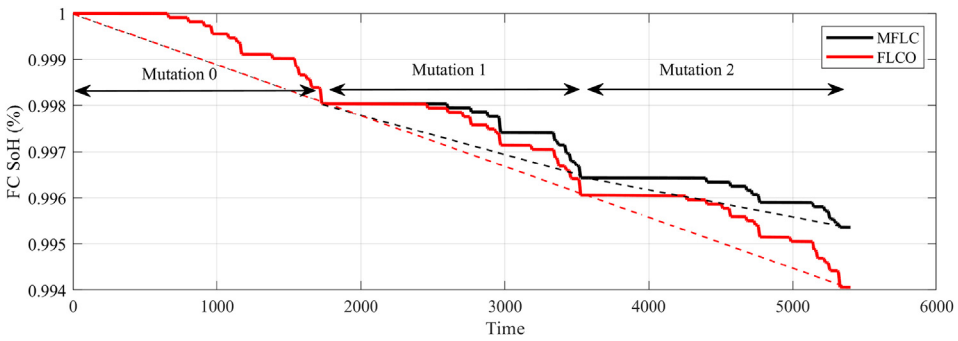

Fig. 10 – Effect of MFLC on reducing fuel cell degradation. The simulation period was three consecutive WLTP Class-3 drive cycles, each with a period of 1800 s. After each drive cycle, a mutation was induced to see the effect of this compared to the last. The gradient of the FC SoH can be seen to decrease with each mutation.

Effect of MFLC on fuel cell lifetime

The MFLC was operated according to the same test conditions previously stated; however, after each drive cycle, the SoD was increased to induce a membership function mutation. The degradation states used were 0, 0.5 and 1 for each drive cycle. Fig. 10 shows the effect each mutation had on FC state-of-health over each drive cycle. The MFLC with no mutations was also operated over three drive cycles to act as a baseline. Due to the FC degradation input membership function, 25% of the FC life will be operated under mutation 0, 50% under mutation 1 and 25% under mutation 2, which resulted in a 32.8% increase in FC lifetime. The trade-off to each mutation would be a reduced peak power output and slower response time to dynamic loads in this case.

The MFLC is not limited to mutations solely from FC degradation. Any number of vehicle parameters could induce a mutation of membership functions, such as FC temperature, battery temperature, or hydrogen tank level.

Please cite this article as: Luca R et al., Comparative study of energy management systems for a hybrid fuel cell electric vehicle - A novel mutative fuzzy logic controller to prolong fuel cell lifetime, International Journal of Hydrogen Energy, https://doi.org/10.1016/j.ijhydene.2022.05.192

Conclusion and future work

An effective energy management system is essential in the successful and long-lasting operation of a hybrid fuel cell battery vehicle. A modelling framework named EV-SimKit has been outlined which allows for the fast comparison of EMSs for a range of vehicle types. ECMS and SMC were found to have a significant impact on fuel cell degradation due to rapid and large load changes. RLP resulted in very low FC degradation due to the nature of the EMS; however, this also meant it rarely operated the FC system at peak efficiency. Both FLCS and FLCO had high FC system efficiency; however, FLCS had a large impact on fuel cell degradation. The optimisation significantly reduced this to 0.028 $/km, which was the second-best of all EMSs. A novel development was then presented on the fuzzy logic controller, whereby the output membership functions were mutated as a result of a calculated quantity named state-of-degradation (SoD). In a real application, this could equally be true degradation, such as reduction in mV at a given current density compared to beginning of life performance. The MFLC was operated at three different states of degradation, and it was shown to increase fuel cell lifetime by 32.8% when operated in the ratio of 1:2:1 for mutation 0, 1 and 2 respectively.

As system degradation is also a function of temperature, future work could include implementing thermal models for the fuel cell and battery pack, a tube and fin radiator with fan and a hydraulic network model for pressure drop and pump power simulation. EV-SimKit can then be validated at a system level.

Declaration of competing interest

The authors declare that they have no known competing financial interests or personal relationships that could have appeared to influence the work reported in this paper.

Acknowledgments

Robert Luca acknowledges a studentship from the EPSRC Centre for Doctoral Training in Fuel Cells and their Fuels (EP/L015749/1) the Electrochemical Innovation Lab (EIL) is supported through EPSRC projects (EP/M014371/1, EP/S018204/2, EP/R023581/1, EP/P009050/1, EP/L015749/1, EP/M009394/1, EP/M023508/1). Paul R. Shearing acknowledges funding from the Royal Academy of Engineering. Shearing and Brett acknowledge the Faraday Institution (EP/S003053/1).

Appendix A. Supplementary data

Supplementary data to this article can be found online at https://doi.org/10.1016/j.ijhydene.2022.05.192.

REFERENCES

[1] I.E.A. (IEA). World energy balances. 2018 [Online]. Available: https://webstore.iea.org/world-energy-balances-2018.
[2] Nykvist B, Sprei F, Nilsson M. Assessing the progress toward lower priced long range battery electric vehicles. Energy Pol 2019;124:144–55. 1 1.
[3] Paladini V, Donateo T, de Risi A, Laforgia D. Control strategy optimization of a fuel-cell electric vehicle. J Fuel Cell Sci Technol 2008;5(2). 5.
[4] Yue M, Jemei S, Gouriveau R, Zerhouni N. Review on health-conscious energy management strategies for fuel cell hybrid electric vehicles: degradation models and strategies. 2019.
[5] Sulaiman N, Hannan MA, Mohamed A, Majlan EH, Wan Daud WR. A review on energy management system for fuel cell hybrid electric vehicle: issues and challenges, vol. 52. Elsevier Ltd; 2015. p. 802–14.
[6] Zuo Wei, Li Qingqing, He Zhu, Li Yawei. Numerical investigations on thermal performance enhancement of hydrogen-fueled micro planar combustors with injectors for micro-thermophotovoltaic applications. Energy 2020;194:116904.
[7] Zuo Wei, Zhang Yuntian, Li Qingqing, Li Jing, He Zhu. Numerical investigations on hydrogen-fueled micro-cylindrical combustors with cavity for micro-thermophotovoltaic applications. Energy 2021;223:120098.
[8] Zuo Wei, Zhao Hongshuo, Jiaqiang E, Li Qingqing, Li Dexin, Yang Di, et al. Effects of injection strategies on thermal performance of a novel micro planar combustor fueled by hydrogen. Int J Hydrogen Energy 2022;47(14):9018–29.
[9] Wu B, Parkes MA, Yufit V, De Benedetti L, Veismann S, Wirsching C, et al. Design and testing of a 9.5 kWe proton exchange membrane fuel cell-supercapacitor passive hybrid system. Int J Hydrogen Energy 2014;39(15):7885–96.
[10] Bernard J, Hofer M, Hannesen U, Toth A, Tsukada A, Büchi FN, Dietrich P. Fuel cell/battery passive hybrid power source for electric powertrains. J Power Sources 2011;196(14):5867–72. 15 7.
[11] Kuperman A, Aharon I, Kara A, Malki S. A frequency domain approach to analyzing passive battery-ultracapacitor hybrids supplying periodic pulsed current loads. Energy Convers Manag 2011;52(12):3433–8. 11.
[12] Chen YS, Lin SM, Hong BS. Experimental study on a passive fuel Cell/Battery hybrid power system. Energies 2013;6(12):6413–22.
[13] Lee SC, Kwon O, Thomas S, Park S, Choi GH. Graphical and mathematical analysis of fuel cell/battery passive hybridization with K factors. Appl Energy 2014;114:135–45.
[14] Whiteley M, Dunnett S, Jackson L. Failure mode and effect analysis, and fault tree analysis of polymer electrolyte membrane fuel cells. Int J Hydrogen Energy 2016;41(2):1187–202. 12 1.
[15] Guilbert D, Mohammadi A, Gaillard A, N'Diaye A, Djerdir A. Interactions between fuel cell and DC/DC converter for fuel cell electric vehicle applications: influence of faults. In: IECON 2013 - 39th annual conference of the IEEE industrial electronics society, vienna; 2013. p. 912–7.
[16] Chen H, Zhao X, Zhang T, Pei P. The reactant starvation of the proton exchange membrane fuel cells for vehicular applications: a review, vol. 182. Elsevier Ltd; 2019. p. 282–98.
[17] Li Jing, Zuo Wei, Jiaqiang E, Zhang Yuntian, Li Qingqing, Sun Ke, Zhou Kun, Zhang Guangde. Multi-objective optimization of mini U-channel cold plate with SiO2 nanofluid by RSM and NSGA-II. Energy 2021:123039.

Please cite this article as: Luca R et al., Comparative study of energy management systems for a hybrid fuel cell electric vehicle - A novel mutative fuzzy logic controller to prolong fuel cell lifetime, International Journal of Hydrogen Energy, https://doi.org/10.1016/j.ijhydene.2022.05.192

[18] Njoya Motapon S, Dessaint LA, Al-Haddad K. A comparative study of energy management schemes for a fuel-cell hybrid emergency power system of more-electric aircraft. IEEE Trans Ind Electron 2014;61(3):1320–34.
[19] Li Q, Wang T, Dai C, Chen W, Ma L. Power management strategy based on adaptive droop control for a fuel cell-battery-supercapacitor hybrid tramway. IEEE Trans Veh Technol 2018;67(7):5658–70. 1 7.
[20] Yue M, Jemei S, Zerhouni N. Health-conscious energy management for fuel cell hybrid electric vehicles based on prognostics-enabled decision-making. IEEE Trans Veh Technol 2019;68(12):11483–91. 1 12.
[21] Ahmadi S, Bathaee SM, Hosseinpour AH. Improving fuel economy and performance of a fuel-cell hybrid electric vehicle (fuel-cell, battery, and ultra-capacitor) using optimized energy management strategy. Energy Convers Manag 2018;160:74–84.
[22] Garcia P, Fernandez LM, Garcia CA, Jurado F. Energy management system of fuel-cell-battery hybrid tramway. IEEE Trans Ind Electron 2010;57(12):4013–23. 12.
[23] Hong Z, Li Q, Han Y, Shang W, Zhu Y, Chen W. An energy management strategy based on dynamic power factor for fuel cell/battery hybrid locomotive. Int J Hydrogen Energy 2018;43(6):3261–72. 8 2.
[24] Zhang X, Liu L, Dai Y, Lu T. Experimental investigation on the online fuzzy energy management of hybrid fuel cell/battery power system for UAVs. Int J Hydrogen Energy 2018;43(21):10094–103.
[25] Hames Y, Kaya K, Baltacioglu E, Turksoy A. Analysis of the control strategies for fuel saving in the hydrogen fuel cell vehicles. Int J Hydrogen Energy 2018;43(23):10810–21. 7 6.
[26] Li H, Ravey A, N'Diaye A, Djerdir A. A novel equivalent consumption minimization strategy for hybrid electric vehicle powered by fuel cell, battery and supercapacitor. J Power Sources 2018;395:262–70. 15 8.
[27] Han J, Park Y, Park YS. A novel updating method of equivalent factor in ECMS for prolonging the lifetime of battery in fuel cell hybrid electric vehicle. In: IFAC proceedings volumes. IFAC-Papers Online; 2012.
[28] Zhang W, Li J, Xu L, Ouyang M. Optimization for a fuel cell/battery/capacity tram with equivalent consumption minimization strategy. Energy Convers Manag 2017;134:59–69.
[29] Opila DF. Equivalent Degradation Minimization Strategy for balancing battery and capacitor usage in hybrid energy storage systems for electric vehicles. Seattle, WA: American Control Conference (ACC); 2017. p. 315–21.
[30] Xu L, Ouyang M, Li J, Yang F, Lu L, Hua J. Application of Pontryagin's Minimal Principle to the energy management strategy of plugin fuel cell electric vehicles. Int J Hydrogen Energy 2013;38(24):10104–15. 12 8.
[31] Chen J, Xu C, Wu C, Xu W. Adaptive fuzzy logic control of fuel-cell-battery hybrid systems for electric vehicles. IEEE Trans Ind Inf 2018;14(1):292–300. 1 1.
[32] Wang Y, Moura SJ, Advani SG, Prasad AK. Power management system for a fuel cell/battery hybrid vehicle incorporating fuel cell and battery degradation. Int J Hydrogen Energy 2019;44(16):8479–92. 29 3.
[33] Ettihir K, Boulon L, Agbossou K. Optimization-based energy management strategy for a fuel cell/battery hybrid power system. Appl Energy 2016;163:142–53. 1 2.
[34] Ou K, Yuan WW, Choi M, Yang S, Jung S, Kim YB. Optimized power management based on adaptive-PMP algorithm for a stationary PEM fuel cell/battery hybrid system. Int J Hydrogen Energy 2018;43(32):15433–44. 9 8.
[35] Solano Martínez J, Mulot J, Harel F, Hissel D, Péra MC, John RI, Amiet M. Experimental validation of a type-2 fuzzy logic controller for energy management in hybrid electrical vehicles. Eng Appl Artif Intell 2013;26(7):1772–9. 8.
[36] Garcia P, Torreglosa JP, Fernandez LM, Jurado F. Control strategies for high-power electric vehicles powered by hydrogen fuel cell, battery and supercapacitor. Expert Systems with Applications; 2013.
[37] Yufit V, Brandon NP. Development and application of an actively controlled hybrid proton exchange membrane fuel cell - lithium-ion battery laboratory test-bed based on off-the-shelf components. J Power Sources 2011;196(2):801–7.
[38] Mi Chris, Abul Masrur M. Hybrid electric vehicles: principles and applications with practical perspectives. John Wiley & Sons; 2017.
[39] Varocky BJ. Benchmarking of regenerative braking for a fully electric car. DC (Diabetol Croat) 2011;2:44. D.
[40] Zheng CH, Oh CE, Park YI, Cha SW. Fuel economy evaluation of fuel cell hybrid vehicles based on equivalent fuel consumption. Int J Hydrogen Energy 2012;37(2):1790–6. 1.
[41] Schweighofer B, Raab KM, Brasseur G. Modeling of high power automotive batteries by the use of an automated test system. IEEE Trans Instrum Meas 2003;52(4):1087–91.
[42] Ahmed R, Gazzarri J, Onori S, Habibi S, Jackey R, Rzemien K, Tjong J, LeSage J. Model-based parameter identification of healthy and aged Li-ion batteries for electric vehicle applications. Source: SAE International Journal of Alternative Powertrains 2015;4(2):233–47.
[43] Pastor-Fernández C, Bruen T, Widanage WD, Gama-Valdez MA, Marco J. A study of cell-to-cell interactions and degradation in parallel strings: implications for the battery management system. J Power Sources 2016;329:574–85. 15 10.
[44] Smith K, Earleywine M, Wood E, Neubauer J, Pesaran A. Comparison of plug-in hybrid electric vehicle battery life across geographies and drive cycles. In: SAE technical papers; 2012.
[45] Smith K, Wood E, Santhanagopalan S, Kim G-H, Neubauer J, Pesaran A. Models for battery reliability and lifetime. 2013.
[46] Lazar AL, Konradt SC, Rottengruber H. Open-source dynamic MATLAb/Simulink 1D proton exchange membrane fuel cell model. Energies 2019;12(18). 9 9.
[47] Kulkarni N, Meyer Q, Hack J, Jervis R, Iacoviello F, Ronaszegi K, Adcock P, Shearing PR, Brett DJ. Examining the effect of the secondary flow-field on polymer electrolyte fuel cells using X-ray computed radiography and computational modelling. Int J Hydrogen Energy 2019;44(2):1139–50. 8 1.
[48] Chaudhary S, Sachan VK, Bhattacharya PK. Two dimensional modelling of water uptake in proton exchange membrane fuel cell. Int J Hydrogen Energy 2014;39(31):17802–18.
[49] Anderson AB, Roques J, Mukerjee S, Murthi VS, Markovic NM, Stamenkovic V. Activation energies for oxygen reduction on platinum alloys: theory and experiment. J Phys Chem B 2005;109(3):1198–203. 27 1.
[50] Hack J, García-Salaberri PA, Kok MDR, Jervis R, Shearing PR, Brandon N, Brett DJL. X-ray micro-computed tomography of polymer electrolyte fuel cells: what is the representative elementary area? J Electrochem Soc 2020;167(1):13545. 22 1.
[51] Kolde JA. Advanced composite polymer electrolyte fuel cell membranes. ECS Proceedings Volumes 1995;1995(1):193–201. 23 1.
[52] Hack J, Heenan TMM, Iacoviello F, Mansor N, Meyer Q, Shearing P, Brandon N, Brett DJL. A structure and durability comparison of membrane electrode assembly fabrication methods: self-assembled versus hot-pressed. J Electrochem Soc 2018;165(6):F3045–52.
[53] Sharaf OZ, Orhan MF. An overview of fuel cell technology: fundamentals and applications, vol. 32; 2014. p. 810–53.

Please cite this article as: Luca R et al., Comparative study of energy management systems for a hybrid fuel cell electric vehicle - A novel mutative fuzzy logic controller to prolong fuel cell lifetime, International Journal of Hydrogen Energy, https://doi.org/10.1016/j.ijhydene.2022.05.192

[54] Kneer A, Wagner N. A semi-empirical catalyst degradation model based on voltage cycling under automotive operating conditions in PEM fuel cells. J Electrochem Soc 2019;166(2):F120–7.
[55] Debe MK, Schmoeckel AK, Vernstrom GD, Atanasoski R. High voltage stability of nanostructured thin film catalysts for PEM fuel cells. J Power Sources 2006;161(2):1002–11. 27 10.
[56] Kneer A, Jankovic J, Susac D, Putz A, Wagner N, Sabharwal M, Secanell M. Correlation of changes in electrochemical and structural parameters due to voltage cycling induced degradation in PEM fuel cells. J Electrochem Soc 2018;165(6):F3241–50.
[57] Pei P, Chang Q, Tang T. A quick evaluating method for automotive fuel cell lifetime. Int J Hydrogen Energy 2008;33(14):3829–36.
[58] Tian T, Tang J, Chen Y, Tan J, Li S, Pan M. Study on accelerated stress test for fuel cell lifetime. Int J Electrochem Sci 2018;13(2):2022–32.
[59] Hicks M, Pierpont D, Turner P, Watschke T. Accelerated testing and lifetime modeling for the development of durable fuel cell MEAs. ECS Trans 2019;1(8):229–37.
[60] Mock P, Kühlwein J, Tietge U, Franco V, Bandivadekar A, German J. The WLTP: how a new test procedure for cars will affect fuel consumption values in the EU. 2014.

Please cite this article as: Luca R et al., Comparative study of energy management systems for a hybrid fuel cell electric vehicle - A novel mutative fuzzy logic controller to prolong fuel cell lifetime, International Journal of Hydrogen Energy, https://doi.org/10.1016/j.ijhydene.2022.05.192